IOP Publishing Inverse Problems

Inverse Problems **41** (2025) 075017 (17pp) https://doi.org/10.1088/1361-6420/adef75

Inverse gravimetry by multipole expansions

Tianshi Lu* **and Santosh Linkha**

Department of Mathematics and Statistics, Wichita State University, Wichita, KS 67260-0033, United States of America

E-mail: tianshi.lu@wichita.edu

Received 20 March 2025; revised 19 June 2025
Accepted for publication 14 July 2025
Published 23 July 2025

Abstract

We introduced a two-step method of multipole expansions for the inverse gravimetry problem in two- and three- dimensions. The source was regularized to be elliptic or rectangular for efficiency and robustness. In the first step, we estimated the center of the source by back tracing the measured gravity fields. In the second step, we solved a linear system with the measured gravity fields to estimate the mass, dipole, and quadruple of the source expanded about the estimated source center, then solved the nonlinear equations for the source parameters. We derived the error bounds for the parameters of the source in the presence of measurement noises. We demonstrated the accuracy and robustness of the method by numerical examples.

Keywords: inverse gravimetry, multipole expansion, error analysis

1. Introduction

The inverse gravimetry problem has been studied for decades [1–4]. Microgravimetric surveying techniques have been utilized to detect natural (see [3, 4]) and man-made (see [5]) underground cavities. The inverse gravimetry problem is severely ill-posed [1]. In this paper, we seek the two- or three- dimensional source Ω with a uniform mass distribution from the gravity field measured at a few points around Ω. The uniqueness of the inverse problem is not guaranteed in general. However, [1] established the uniqueness for sources that is either star-shaped with respect to its center of gravity or convex in one direction. Isakov [1] also proved the logarithmic-type stability estimate for star-shaped sources.

Level set method has been studied to recover the source from partial data [2, 6]. The linear mapping from the source to the gravity field around it has exponentially fast decreasing singular values [6]. It was demonstrated in [7] that one could only expect to find four to seven parameters describing the source. Recently, Isakov and Titi proposed to use the multipole expansion to solve the inverse gravimetry problem for two-dimensional sources in [8] and extended the

* Author to whom any correspondence should be addressed.

method to simplified three-dimensional sources in [9]. For the level set method, the gravity field was measured on a mesh in a manifold around Ω, and the source was reconstructed by solving a PDE. In contract, the gravity field only need to be measured at a few scattered points around Ω for the multipole expansion method, and the reconstruction of the source is a mostly linear process, which is highly efficient and more feasible for the error analysis.

Our inverse gravimetry problem seeks the domain Ω of the source with uniform density in $\mathbb{R}^2$ or $\mathbb{R}^3$ from the gravity fields measured at a few points around Ω. Since the domain is not uniquely determined by discrete data, we regularize the domain to be either elliptic or rectangular as in [8, 9]. The gravity field is a nonlinear function of the location and shape of the source domain. The inverse problem can be solved by an iterative solver such as the gradient descent method. However, the gravity fields for a three-dimensional source are calculated by triple integrals, which are computationally expensive, even with the fast implementation using polar coordinates [2] or low rank approximation [6]. Moreover, it is hard to analyze the error and convergence of the iterative solver, and it may lead to spurious solutions. Instead we use the multipole expansion of the gravity field, which gives a system of linear equations, to find the approximate geometry of the source. The non-iterative solver is efficient and gives a unique solution with provable error bounds.

We adopt the following notations in the paper. The dimension of the source is denoted by d. The vector $\mathbf{g}(\mathbf{r})$ denotes the exact gravity field at $\mathbf{r}$ and $\mathbf{g}_i$ denotes the measured gravity field at $\mathbf{r}_i$ with possible noise. The vector $\mathbf{r}_c$ denotes the center of gravity of the source. $R = \min_{1\leqslant i\leqslant N}\|\mathbf{r}_i\|$ and $R_c = \min_{1\leqslant i\leqslant N}\|\mathbf{r}_i - \mathbf{r}_c\|$ are the minimum distance from the measuring points to the origin and $\mathbf{r}_c$. For a vector $\mathbf{r}$, $r = \|\mathbf{r}\|$ and $\hat{\mathbf{r}} = \mathbf{r}/r$. For a parameter p, $\tilde{p}$ is the estimated value of p from the measured gravity fields, and $\delta p = \tilde{p} - p$.

In section 2, we generalize the method of multipole expansion in [8, 9] and introduce a two-step method of multipole expansion for 2D and 3D inverse gravimetry problems. In section 3, we derive the error bounds for each step in the proposed method in the presence of noises in the measurements. In section 4, we demonstrated the accuracy and robustness of the algorithm by numerical examples. In section 5, we make comments and draw conclusions.

2. Algorithm for inverse gravimetry

2.1. Two-dimensional multipole expansion

Following [8], we study the inverse gravimetry problem in two dimensions. The source is regularized to be an ellipse or a rectangle due to the presence of the background noise in the measurements. We measure the gravity at a few points around the source and infer the geometry of the source from the measurements. Let $\phi(\mathbf{r})$ be the gravitational potential of a uniform source in a domain $\Omega \subset \mathbb{R}^2$,

$$\phi(\mathbf{r}) = -\int_\Omega \ln\|\mathbf{r} - \mathbf{r}'\|\mathrm{d}\mathbf{r}'.$$

For convenience the density of the source is set to -2π. The negative density represents a cavity, which is common for inverse gravimetry. The multipole expansion

about the origin gives

$$-\ln\|\mathbf{r}-\mathbf{r}'\| = -\ln r + \sum_{l=1}^{\infty} \frac{\|\mathbf{r}'\|^l}{lr^l}\cos\left(l(\theta-\theta')\right) = -\ln r + \frac{\hat{\mathbf{r}}^{\mathrm{T}}\mathbf{r}'}{r} + \frac{2\left(\hat{\mathbf{r}}^{\mathrm{T}}\mathbf{r}'\right)^2 - \|\mathbf{r}'\|^2}{2r^2} + O\left(r^{-3}\right), \tag{1}$$

where $r=\|\mathbf{r}\|$, $\hat{\mathbf{r}}=\mathbf{r}/r$, θ and θ' are the azimuthal angle of $\mathbf{r}$ and $\mathbf{r}'$ respectively. Let

$$M=\int_{\Omega}\mathrm{d}\mathbf{r}', \quad \mathbf{p}=\int_{\Omega}\mathbf{r}'\mathrm{d}\mathbf{r}', \quad Q=\int_{\Omega}\left(2\mathbf{r}'\mathbf{r}'^{\mathrm{T}}-\|\mathbf{r}'\|^2 I\right)\mathrm{d}\mathbf{r}',$$

be the first three harmonic moments. Then

$$\phi(\mathbf{r}) = -M\ln r + \frac{\hat{\mathbf{r}}^{\mathrm{T}}\mathbf{p}}{r} + \frac{\hat{\mathbf{r}}^{\mathrm{T}}Q\hat{\mathbf{r}}}{2r^2} + O\left(r^{-3}\right).$$

The gravity at $\mathbf{r}$ is

$$\mathbf{g}(\mathbf{r}) = -\nabla\phi(\mathbf{r}) = \frac{M\hat{\mathbf{r}}}{r} + \frac{2\hat{\mathbf{r}}\hat{\mathbf{r}}^{\mathrm{T}}\mathbf{p}-\mathbf{p}}{r^2} + \frac{2\hat{\mathbf{r}}\hat{\mathbf{r}}^{\mathrm{T}}Q\hat{\mathbf{r}}-Q\hat{\mathbf{r}}}{r^3} + O\left(r^{-4}\right). \tag{2}$$

Noticing that Q is symmetric and $\mathrm{Tr}Q=0$, we set $\mathbf{q}=(Q_{11},Q_{12})^{\mathrm{T}}$ as the free parameters of Q. There are five multipole parameters of the source, namely, $(M;\mathbf{p};\mathbf{q})$, where the semicolons represent vertical concatenation. Denote the gravity fields measured at the N points $\{\mathbf{r}_1,\cdots,\mathbf{r}_N\}$ by $\{\mathbf{g}_1,\cdots,\mathbf{g}_N\}$. We introduce the auxiliary vector that has the dimension of the gravity field,

$$\mathbf{v}=\left(M/R,\mathbf{p}/R^2,\mathbf{q}/R^3\right),$$

where $R=\min_{1\leqslant i\leqslant N}\|\mathbf{r}_i\|$. The estimated multipole parameters are given by the least squares solution to the linear system

$$A\tilde{\mathbf{v}}=\mathbf{g}\equiv(\mathbf{g}_1;\cdots;\mathbf{g}_N), \tag{3}$$

where A is a dimensionless $2N\times 5$ matrix that satisfies

$$A\mathbf{v}=\mathbf{g}_Q\equiv\left(\mathbf{g}_Q(\mathbf{r}_1);\cdots;\mathbf{g}_Q(\mathbf{r}_N)\right),$$

where

$$\mathbf{g}_Q(\mathbf{r}) = \frac{M\hat{\mathbf{r}}}{r} + \frac{2\hat{\mathbf{r}}\hat{\mathbf{r}}^{\mathrm{T}}\mathbf{p}-\mathbf{p}}{r^2} + \frac{2\hat{\mathbf{r}}\hat{\mathbf{r}}^{\mathrm{T}}Q\hat{\mathbf{r}}-Q\hat{\mathbf{r}}}{r^3},$$

in which Q is determined by $\mathbf{q}$. We assume $\mathrm{rank}(A)=5$, so that it has a unique least squares solution $\tilde{\mathbf{v}}=A^{+}\mathbf{g}$, where A^{+} is the pseudoinverse of A.

An ellipse or a rectangle has five free parameters, namely, the center $\mathbf{r}_c$, the half axes $\mathbf{a}=(a_1,a_2)$ with $a_1\geqslant a_2$, and the azimuthal angle of the first half axis $\alpha_1\in(-\pi/2,\pi/2]$. There is a one-to-one mapping from $\{\mathbf{r}_c,\mathbf{a},\alpha_1\}$ to $\{M,\mathbf{p},\mathbf{q}\}$, except for the case $a_1=a_2$ for which α_1 is arbitrary. We estimate $\{\mathbf{r}_c,\mathbf{a},\alpha_1\}$ by applying the inverse mapping to $\{\tilde{M},\tilde{\mathbf{p}},\tilde{\mathbf{q}}\}$. The estimated

center of the cavity is $\tilde{\mathbf{r}}_c = \tilde{\mathbf{p}}/\tilde{M}$, from which we compute the quadruple relative to the center of the source,

$$\tilde{Q}_r = \tilde{Q} - \tilde{M}\left(2\tilde{\mathbf{r}}_c\tilde{\mathbf{r}}_c^{\mathrm{T}} - \|\tilde{\mathbf{r}}_c\|^2 I\right).$$

For an elliptic or rectangular cavity,

$$(Q_r)_{11} = \frac{M}{c_Q}\left(a_1^2 - a_2^2\right)\cos\left(2\alpha_1\right), \quad (Q_r)_{12} = \frac{M}{c_Q}\left(a_1^2 - a_2^2\right)\sin\left(2\alpha_1\right),$$

where c_Q is 4 for an elliptic cavity and 3 for a rectangular cavity. We can estimate $a_1^2 - a_2^2$ and α_1 by

$$\tilde{a}_1^2 - \tilde{a}_2^2 = \frac{c_Q}{\tilde{M}}\sqrt{\left(\tilde{Q}_r\right)_{11}^2 + \left(\tilde{Q}_r\right)_{12}^2}, \quad \tilde{\alpha}_1 = \frac{1}{2}\arg\left(\left(\tilde{Q}_r\right)_{11} + i\left(\tilde{Q}_r\right)_{12}\right).$$

The product of two half-axes, a_1a_2, is estimated by $\tilde{M}/\pi$ for an ellipse and $\tilde{M}/4$ for a rectangle. By the identity

$$\|\mathbf{a}\|^2 = \sqrt{\left(a_1^2 - a_2^2\right)^2 + 4\left(a_1a_2\right)^2},$$

we can estimate the value of $\|\mathbf{a}\|^2$, and then a_1 and a_2.

2.2. *Three-dimensional multipole expansion*

We generalize the method for three dimensional sources in [9]. For a 3D source with uniform density of -4π, the gravitational potential is

$$\phi(\mathbf{r}) = \int_\Omega \frac{1}{\|\mathbf{r} - \mathbf{r}'\|}\mathrm{d}\mathbf{r}'.$$

The multipole expansion is

$$\frac{1}{\|\mathbf{r} - \mathbf{r}'\|} = \sum_{l=0}^{\infty}\frac{\|\mathbf{r}'\|^l}{r^{l+1}}P_l\left(\hat{\mathbf{r}}\cdot\hat{\mathbf{r}}'\right) = \frac{1}{r} + \frac{\hat{\mathbf{r}}^{\mathrm{T}}\mathbf{r}'}{r^2} + \frac{3\left(\hat{\mathbf{r}}^{\mathrm{T}}\mathbf{r}'\right)^2 - \|\mathbf{r}'\|^2}{2r^3} + O\left(r^{-4}\right), \tag{4}$$

where P_l is the Legendre polynomial. In terms of the first three harmonic moments,

$$M = \int_\Omega \mathrm{d}\mathbf{r}', \quad \mathbf{p} = \int_\Omega \mathbf{r}'\mathrm{d}\mathbf{r}', \quad Q = \int_\Omega\left(3\mathbf{r}'\mathbf{r}'^{\mathrm{T}} - \|\mathbf{r}'\|^2 I\right)\mathrm{d}\mathbf{r}',$$

$$\phi(\mathbf{r}) = \frac{M}{r} + \frac{\hat{\mathbf{r}}^{\mathrm{T}}\mathbf{p}}{r^2} + \frac{\hat{\mathbf{r}}^{\mathrm{T}}Q\hat{\mathbf{r}}}{2r^3} + O\left(r^{-4}\right),$$

$$\mathbf{g}(\mathbf{r}) = -\nabla\phi(\mathbf{r}) = \frac{M\hat{\mathbf{r}}}{r^2} + \frac{3\hat{\mathbf{r}}\hat{\mathbf{r}}^{\mathrm{T}}\mathbf{p} - \mathbf{p}}{r^3} + \frac{5\hat{\mathbf{r}}\hat{\mathbf{r}}^{\mathrm{T}}Q\hat{\mathbf{r}} - 2Q\hat{\mathbf{r}}}{2r^4} + O\left(r^{-5}\right). \tag{5}$$

Since Q is symmetric and $\mathrm{Tr}Q = 0$, we set $\mathbf{q} = (Q_{11}, Q_{22}, Q_{12}, Q_{13}, Q_{23})^{\mathrm{T}}$ as the free parameters of Q. With the auxiliary vector

$$\mathbf{v} = \left(M/R^2, \mathbf{p}/R^3, \mathbf{q}/R^4\right),$$

where $R = \min_{1\leqslant i\leqslant N} \|\mathbf{r}_i\|$, the nine multipole parameters of the source can be estimated by the least squares solution to the linear system

$$A\tilde{\mathbf{v}} = \mathbf{g} \equiv (\mathbf{g}_1; \cdots; \mathbf{g}_N), \tag{6}$$

where A is a dimensionless $3N \times 9$ matrix that satisfies

$$A\mathbf{v} = \left(\mathbf{g}_Q(\mathbf{r}_1); \cdots; \mathbf{g}_Q(\mathbf{r}_N)\right),$$

where

$$\mathbf{g}_Q(\mathbf{r}) = \frac{M\hat{\mathbf{r}}}{r^2} + \frac{3\hat{\mathbf{r}}\hat{\mathbf{r}}^{\mathrm{T}}\mathbf{p} - \mathbf{p}}{r^3} + \frac{5\hat{\mathbf{r}}\hat{\mathbf{r}}^{\mathrm{T}}Q\hat{\mathbf{r}} - 2Q\hat{\mathbf{r}}}{2r^4}.$$

We assume $\operatorname{rank}(A) = 9$, so that it has a unique least squares solution $\tilde{\mathbf{v}} = A^{+}\mathbf{g}$, where A^{+} is the pseudoinverse of A.

Assume the source is an ellipsoid or a rectangular prism. Let $\mathbf{a} = (a_1, a_2, a_3)$ with $a_1 \geqslant a_2 \geqslant a_3$ and $U = (\mathbf{u}_1, \mathbf{u}_2, \mathbf{u}_3)$ be an orthogonal matrix such that $\{a_1\mathbf{u}_1, a_2\mathbf{u}_2, a_3\mathbf{u}_3\}$ are the three half axes of Ω. We estimate $\{\mathbf{r}_c, \mathbf{a}, U\}$, which has nine degrees of freedom, from $\{\tilde{M}, \tilde{\mathbf{p}}, \tilde{\mathbf{q}}\}$. The estimated center is $\tilde{\mathbf{r}}_c = \tilde{\mathbf{p}}/\tilde{M}$, from which we estimate the quadruple relative to the center,

$$\tilde{Q}_r = \tilde{Q} - \tilde{M}\left(3\tilde{\mathbf{r}}_c\tilde{\mathbf{r}}_c^{\mathrm{T}} - \|\tilde{\mathbf{r}}_c\|^2 I\right).$$

With $c_Q = 5$ for an ellipsoid and $c_Q = 3$ for a rectangular prism,

$$Q_r = \frac{M}{c_Q} U\left(3D - \|\mathbf{a}\|^2 I\right) U^{\mathrm{T}},$$

where $D = \operatorname{diag}(a_1^2, a_2^2, a_3^2)$. Diagonalizing $c_Q\tilde{Q}_r/\tilde{M}$, we estimate $\mathbf{u}_i$'s by the eigenvectors and $\lambda_i \equiv 3a_i^2 - \|\mathbf{a}\|^2$ by the eigenvalues. The product of three half-axes, $P = a_1a_2a_3$, is estimated by $3\tilde{M}/(4\pi)$ for an ellipsoid and $\tilde{M}/8$ for a rectangular prism. We approximate $\|\mathbf{a}\|^2$ by the unique root to the cubic equation

$$(x + \lambda_1)(x + \lambda_2)(x + \lambda_3) = 27P^2,$$

that satisfies $x \geqslant -\lambda_i$ for $1 \leqslant i \leqslant 3$. Explicitly,

$$\|\mathbf{a}\|^2 = \sqrt[3]{\frac{q}{2} + \sqrt{\frac{q^2}{4} + \frac{p^3}{27}}} + \sqrt[3]{\frac{q}{2} - \sqrt{\frac{q^2}{4} + \frac{p^3}{27}}},$$

where $p = \lambda_1\lambda_2 + \lambda_2\lambda_3 + \lambda_3\lambda_1$, $q = 27P^2 - \lambda_1\lambda_2\lambda_3$. Lastly, we recover the half-axes by $a_i = \sqrt{(\|\mathbf{a}\|^2 + \lambda_i)/3}$.

2.3. Center of the multipole expansion

The multipole expansion is accurate only if the size of source and the distance from its center to the center of the expansion are both small compared to R, the minimum distance from the measuring points to the center of the expansion. If we set the origin to be the center of the multipole expansion as in [8], the relative error in the quadruple expansion is at least of order $\|\mathbf{r}_c\|^3/R^3$ (cf equation (10)), which gives a relative error of order $\|\mathbf{r}_c\|^3/(a_1^2R)$

(cf equations (11) and (12)) in the estimated half axes. For a small source relatively far away from the origin ($\|\mathbf{r}_c\|/a_1 \gg 1$), the reconstructed source size has large error.

We call the multipole expansion about the origin the one-step method. To reduce the error in the multipole expansion, we propose a two-step method. First we estimate the center of the source by back tracing the measured gravity fields, then we reconstruct the elliptical or rectangular source by the multipole expansion about the estimated center of the source.

Denote $R_c = \min_{1\leqslant i\leqslant N}\|\mathbf{r}_i - \mathbf{r}_c\|$. For a_1 smaller than R_c, the direction of $\mathbf{r}_i - \mathbf{r}_c$ is close to that of the measured field $\mathbf{g}_i$ for $1 \leqslant i \leqslant N$. So $\mathbf{r}_c$ is close to the line L_i defined by $\mathbf{r}(t) = \mathbf{r}_i + \mathbf{g}_i t$ for $1 \leqslant i \leqslant N$. We estimate $\mathbf{r}_c$ to be the point that minimizes

$$f(\mathbf{r}_c) = \sum_{i=1}^{N} \operatorname{dist}(\mathbf{r}_c, L_i)^2 .$$

By setting the gradient of $f(\cdot)$ to zero, we see that the estimated $\mathbf{r}_c$, denoted by $\mathbf{r}_{c0}$, satisfies

$$\sum_{i=1}^{N} \left(I - \hat{\mathbf{g}}_i \hat{\mathbf{g}}_i^{\mathrm{T}}\right) \mathbf{r}_{c0} = \sum_{i=1}^{N} \left(I - \hat{\mathbf{g}}_i \hat{\mathbf{g}}_i^{\mathrm{T}}\right) \mathbf{r}_i, \tag{7}$$

where $\hat{\mathbf{g}}_i = \mathbf{g}_i/\|\mathbf{g}_i\|$. The approximate center $\mathbf{r}_{c0}$ is uniquely determined so long as the N fields $\mathbf{g}_i$ are not all parallel. We will show that $\mathbf{r}_{c0}$ is close to the actual center of the source $\mathbf{r}_c$, so that the multipole expansion about $\mathbf{r}_{c0}$ has a small error.

3. Error analysis

We find the error bounds for the geometric parameters of the source computed by the one-step and two-step methods. We assume the noise level is ϵ_n, i.e. for $1 \leqslant i \leqslant N$,

$$\|\mathbf{g}_i - \mathbf{g}(\mathbf{r}_i)\| \leqslant \epsilon_n \|\mathbf{g}(\mathbf{r}_i)\|. \tag{8}$$

Throughout the paper, we simplify $\|A^+\|_\infty$ as $\|A^+\|$. Denote by U the orthogonal matrix composed of the unit vectors along the half-axes.

3.1. Error bounds for the one-step method

Theorem 3.1. *Assume that $\|\mathbf{r}_c\| + a_1 < R$. For the one-step method, the error bounds of M and $\mathbf{r}_c$ are*

$$\frac{|\delta M|}{M} = \|A^+\| O(\epsilon), \quad \frac{\|\delta \mathbf{r}_c\|}{a_1} = \frac{R}{a_1}\|A^+\| O(\epsilon). \tag{9}$$

where

$$\epsilon = \frac{\|\mathbf{r}_c\|\left(\|\mathbf{r}_c\|^2 + a_1^2\right)}{R^3} + \frac{a_1^4}{R^4} + \epsilon_n. \tag{10}$$

For a 2D source, the error bounds of $\mathbf{a}$ *and* U *are*

$$\frac{\|\delta \mathbf{a}\|}{a_1} = \frac{R^2}{a_1^2}\|A^+\| O(\epsilon), \quad \|\delta U\| = \frac{R^2}{a_1^2 - a_2^2}\|A^+\| O(\epsilon). \tag{11}$$

For a 3D source, the error bounds of $\mathbf{a}$ *and* U *are*

$$\frac{\|\delta\mathbf{a}\|}{a_1} = \frac{R^2}{a_1 a_2}\|A^+\| O(\epsilon), \quad \|\delta U\| = \left(\frac{R^2}{a_1^2 - a_2^2} + \frac{R^2}{a_2^2 - a_3^2}\right)\|A^+\| O(\epsilon). \tag{12}$$

Proof. We compute the error of the multiple expansion about the origin. For a 2D source, by equation (1),

$$\mathbf{g}(\mathbf{r}) - \mathbf{g}_Q(\mathbf{r}) = -\nabla \int_\Omega \sum_{l=3}^{\infty} \frac{\|\mathbf{r}'\|^l}{l r^l} \cos(l(\theta - \theta'))\, \mathrm{d}\mathbf{r}'.$$

The octuple term, which vanishes for a symmetric source centered at the origin, is bounded by

$$\left\| \nabla \int_\Omega \frac{\|\mathbf{r}'\|^3}{3r^3} \cos(3(\theta - \theta'))\, \mathrm{d}\mathbf{r}' \right\| = O\left(M \frac{\|\mathbf{r}_c\| \left(\|\mathbf{r}_c\|^2 + a_1^2\right)}{r^4} \right).$$

The 16-tuple term is bounded by

$$\left\| \nabla \int_\Omega \frac{\|\mathbf{r}'\|^4}{4r^4} \cos(4(\theta - \theta'))\, \mathrm{d}\mathbf{r}' \right\| = O\left(M \frac{\left(\|\mathbf{r}_c\|^2 + a_1^2\right)^2}{r^5} \right).$$

The sum of the remaining terms is bounded by

$$\begin{aligned} \sum_{l=5}^{\infty} \int_\Omega \|\mathbf{r}'\|^l \left\| \nabla \frac{\cos(l(\theta - \theta'))}{l r^l} \right\| \mathrm{d}\mathbf{r}' &= \sum_{l=5}^{\infty} \int_\Omega \frac{\|\mathbf{r}'\|^l}{r^{l+1}} \mathrm{d}\mathbf{r}' \leqslant \sum_{l=5}^{\infty} \frac{M}{r} \frac{\left(\|\mathbf{r}_c\| + a_1\right)^l}{r^l} \\ &= \frac{M\left(\|\mathbf{r}_c\| + a_1\right)^5}{\left(r - \|\mathbf{r}_c\| - a_1\right) r^5}. \end{aligned}$$

Since $(\|\mathbf{r}_c\| + a_1)/R < 1$,

$$\|\mathbf{g}(\mathbf{r}) - \mathbf{g}_Q(\mathbf{r})\| = \|\mathbf{g}(\mathbf{r})\| \cdot O\left(\frac{\|\mathbf{r}_c\| \left(\|\mathbf{r}_c\|^2 + a_1^2\right)}{r^3} + \frac{a_1^4}{r^4} \right).$$

Combined with equation (8), for $1 \leqslant i \leqslant N$,

$$\|\mathbf{g}_i - \mathbf{g}_Q(\mathbf{r}_i))\| = \|\mathbf{g}(\mathbf{r}_i)\| \cdot O(\epsilon), \tag{13}$$

where ϵ is given by equation (10). By equation (3), $\tilde{\mathbf{v}} - \mathbf{v} = A^+(\mathbf{g} - \mathbf{g}_Q)$, so

$$\|\tilde{\mathbf{v}} - \mathbf{v}\|_\infty \leqslant \|A^+\|_\infty \|\mathbf{g} - \mathbf{g}_Q\|_\infty = \|A^+\|_\infty M R^{-1} O(\epsilon).$$

which implies

$$\begin{aligned} &|\tilde{M} - M| = M\|A^+\| O(\epsilon), \quad \|\tilde{\mathbf{p}} - \mathbf{p}\| = MR\|A^+\| O(\epsilon), \\ &\|\tilde{\mathbf{q}} - \mathbf{q}\| = MR^2\|A^+\| O(\epsilon). \end{aligned}$$

It follows that the error bounds for M and $\mathbf{r}_c$ are given by equation (9). Since $\|\delta Q\| = MR^2\|A^+\|O(\epsilon)$, $\|\delta Q_r\| = MR^2\|A^+\|O(\epsilon)$ and $\delta(a_1^2 - a_2^2) = R^2\|A^+\|O(\epsilon)$. Since M is proportional to $a_1 a_2$, $\delta(a_1 a_2) = a_1 a_2\|A^+\|O(\epsilon)$. We can obtain δa_1 and δa_2 from the two equations

above. Combined with $\|\delta U\| = O(\|\delta Q_r\|/\|Q_r\|)$, we get the error bounds for $\mathbf{a}$ and U as in equation (11).

For a 3D source, by equation (4),

$$\mathbf{g}(\mathbf{r}) - \mathbf{g}_Q(\mathbf{r}) = -\nabla \int_\Omega \sum_{l=3}^{\infty} \frac{\|\mathbf{r}'\|^l}{r^{l+1}} P_l(\hat{\mathbf{r}} \cdot \hat{\mathbf{r}}')\, \mathrm{d}\mathbf{r}'.$$

Since

$$\left\| \nabla \frac{P_l(\hat{\mathbf{r}} \cdot \hat{\mathbf{r}}')}{r^{l+1}} \right\| = \frac{l+1}{r^{l+2}} \sqrt{(P_l(\hat{\mathbf{r}} \cdot \hat{\mathbf{r}}'))^2 + \frac{\left(1 - (\hat{\mathbf{r}} \cdot \hat{\mathbf{r}}')^2\right)(P_l'(\hat{\mathbf{r}} \cdot \hat{\mathbf{r}}'))^2}{(l+1)^2}} \leqslant \frac{l+1}{r^{l+2}},$$

which can be proved using the limits,

$$\lim_{l\to\infty} P_l(\cos(x/l)) = J_0(x), \quad \lim_{l\to\infty} \frac{\sin(x/l) P_l'(\cos(x/l))}{l+1} = J_1(x),$$

and the inequality $J_0^2(x) + J_1^2(x) \leqslant 1$, where $J_0(\cdot)$ and $J_1(\cdot)$ are the Bessel functions, the sum of the 32-tuple term and beyond is bounded by

$$\begin{aligned} \sum_{l=5}^{\infty} \int_\Omega \|\mathbf{r}'\|^l \left\| \nabla \frac{P_l(\hat{\mathbf{r}} \cdot \hat{\mathbf{r}}')}{r^{l+1}} \right\| \mathrm{d}\mathbf{r}' &\leqslant \sum_{l=5}^{\infty} \frac{M}{r^2} \frac{(\|\mathbf{r}_c\| + a_1)^l (l+1)}{r^l} \\ &= \frac{M(\|\mathbf{r}_c\| + a_1)^5}{(r - \|\mathbf{r}_c\| - a_1)^2 r^5} \left(6 - 5\frac{\|\mathbf{r}_c\| + a_1}{r}\right). \end{aligned}$$

Equation (13) still holds, which gives the error bounds for M and $\mathbf{r}_c$ in equation (9). Since $\|\delta Q_r\| = MR^2\|A^+\|O(\epsilon)$, $\delta(2a_1^2 - a_2^2 - a_3^2) = R^2\|A^+\|O(\epsilon)$ and $\delta(2a_2^2 - a_1^2 - a_3^2) = R^2\|A^+\|O(\epsilon)$. Since M is proportional to $a_1a_2a_3$, $\delta(a_1a_2a_3) = a_1a_2a_3\|A^+\|O(\epsilon)$. Noticing that

$$\|\delta U\| = O\left(\sum_{1\leqslant i<j\leqslant 3} \frac{\|\delta Q_r\|}{|\lambda_i - \lambda_j|} \right),$$

where λ_i's are the eigenvalues of Q_r, we obtain the the error bounds for $\mathbf{a}$ and U in equation (12). The estimated half axes may have large errors if $a_1 \gg a_2$. □

3.2. *Uniqueness of the solution to the linear system*

For a 2D source, there are five parameters, so the minimum number of measuring points is three. By [8], the 6×5 matrix A defined in equation (3) for any 3 distinct points has full rank, so equation (3) has a unique least squares solution for three or more measurements. For a 3D source, there are nine parameters, so the minimum number of measuring points is also three. However, the 9×9 matrix A defined in equation (6) for three distinct points is not always full rank. In fact, A is singular for any three distinct points with the same distance to the center of

the multipole expansion, which will be shown below. W.l.o.g., assume $\|\mathbf{r}_i\| = 1$ for $i = 1,2,3$. The linear system is

$$\left(M + 3\mathbf{r}_i^{\mathrm{T}}\mathbf{p} + \frac{5}{2}\mathbf{r}_i^{\mathrm{T}}Q\mathbf{r}_i\right)\mathbf{r}_i - \mathbf{p} - Q\mathbf{r}_i = \mathbf{g}(\mathbf{r}_i), \quad i = 1,2,3.$$

Denote the circumcenter of the three points $\mathbf{r}_1$, $\mathbf{r}_2$ and $\mathbf{r}_3$ by $h\mathbf{n}$, where $h \geqslant 0$ and $\mathbf{n}$ is a unit vector perpendicular to the plane going through the three points. Let

$$M = -\frac{1+h^2}{2}, \quad \mathbf{p} = h\mathbf{n}, \quad Q = \frac{I}{3} - \mathbf{n}\mathbf{n}^{\mathrm{T}}. \tag{14}$$

It follows that for $i = 1,2,3$, $\mathbf{r}_i^{\mathrm{T}}\mathbf{p} = h^2$, $Q\mathbf{r}_i = \mathbf{r}_i/3 - \mathbf{p}$, and

$$\left(M + 3\mathbf{r}_i^{\mathrm{T}}\mathbf{p} + \frac{5}{2}\mathbf{r}_i^{\mathrm{T}}Q\mathbf{r}_i\right)\mathbf{r}_i - \mathbf{p} - Q\mathbf{r}_i = \left(-\frac{1+h^2}{2} + 3h^2 + \frac{5}{2}\left(\frac{1}{3} - h^2\right)\right) \times \mathbf{r}_i - \mathbf{p} - \left(\frac{\mathbf{r}_i}{3} - \mathbf{p}\right) = 0.$$

It shows that the homogeneous linear system has a nontrivial solution. Furthermore, since equation (14) only depends on $h\mathbf{n}$, $\operatorname{rank}(A) < 9$ for any number of measuring points that are coplanar and have the same distance to the center of the expansion. There are other cases the lead to a rank deficient matrix A. For example, for the three measuring points $\{\mathbf{e}_1, \mathbf{e}_1 + s\mathbf{e}_2, \mathbf{e}_1 - s\mathbf{e}_2\}$ where $\mathbf{e}_1 = (1,0,0)$, $\mathbf{e}_2 = (0,1,0)$, the matrix A is singular for any s.

On the other hand, there are various configurations of measuring points that give a full rank A. For example, for the three measuring points $\{\mathbf{e}_1, \mathbf{e}_1 + s\mathbf{e}_2, \mathbf{e}_1 - 2s\mathbf{e}_2\}$ where $0 < s < 0.3$, the smallest singular value of A satisfies $\sigma_{\min}(A) \geqslant 0.5s^3$, which implies that A is nonsingular. As another example, for the five measuring points $\{\mathbf{e}_1, \mathbf{e}_1 + \mathbf{d}_1, \mathbf{e}_1 - \mathbf{d}_1, \mathbf{e}_1 + \mathbf{d}_2, \mathbf{e}_1 - \mathbf{d}_2\}$ where $\mathbf{d}_1$ and $\mathbf{d}_2$ are arbitrary orthogonal vectors with length up to 0.3, it can be verified that $\sigma_{\min}(A) \geqslant 0.3\|\mathbf{d}_1\| \cdot \|\mathbf{d}_2\|$, therefore A is a full rank matrix.

3.3. Error bound of $\mathbf{r}_{c0}$

Theorem 3.2. *Assume there exists $K > 0$ such that*

$$\frac{1}{N^2}\sum_{i=1}^{N}\sum_{j=1}^{N}\left(1 - \left(\hat{\mathbf{g}}_i^{\mathrm{T}}\hat{\mathbf{g}}_j\right)^2\right) > K. \tag{15}$$

The error bound of the estimated source center is

$$\|\mathbf{r}_{c0} - \mathbf{r}_c\| = R_c \cdot O\left(\frac{a_1^2}{R_c^2} + \epsilon_n\right), \tag{16}$$

where $R_c = \min_{1 \leqslant i \leqslant N}\|\mathbf{r}_i - \mathbf{r}_c\|$.

Proof. Taking the multipole expansion about $\mathbf{r}_c$, which has no dipole term, we obtain from equations (2) and (5) that

$$\left\|\mathbf{g}(\mathbf{r}_c + \mathbf{r}) - \frac{M\hat{\mathbf{r}}}{r^{d-1}}\right\| = \frac{M}{r^{d-1}}O\left(\frac{a_1^2}{r^2}\right).$$

Combined with equation (8), for $1 \leqslant i \leqslant N$,

$$\left\| \hat{\mathbf{g}}_i - \frac{\mathbf{r}_i - \mathbf{r}_c}{\|\mathbf{r}_i - \mathbf{r}_c\|} \right\| = O\left(\frac{a_1^2}{R_c^2} + \epsilon_n\right).$$

As a result,

$$\begin{aligned}\left\| \frac{1}{N}\sum_{i=1}^{N} \left(I - \hat{\mathbf{g}}_i\hat{\mathbf{g}}_i^{\mathrm{T}}\right)(\mathbf{r}_i - \mathbf{r}_c) \right\| &= \left\| \frac{1}{N}\sum_{i=1}^{N} \left(I - \hat{\mathbf{g}}_i\hat{\mathbf{g}}_i^{\mathrm{T}}\right)\|\mathbf{r}_i - \mathbf{r}_c\| \left(\frac{\mathbf{r}_i - \mathbf{r}_c}{\|\mathbf{r}_i - \mathbf{r}_c\|} - \hat{\mathbf{g}}_i\right) \right\| \\ &= R_c \cdot O\left(\frac{a_1^2}{R_c^2} + \epsilon_n\right).\end{aligned}$$

By equation (7),

$$P(\mathbf{r}_{c0} - \mathbf{r}_c) = \frac{1}{N}\sum_{i=1}^{N} \left(I - \hat{\mathbf{g}}_i\hat{\mathbf{g}}_i^{\mathrm{T}}\right)(\mathbf{r}_i - \mathbf{r}_c),$$

where

$$P = \frac{1}{N}\sum_{i=1}^{N} \left(I - \hat{\mathbf{g}}_i\hat{\mathbf{g}}_i^{\mathrm{T}}\right).$$

For any unit vector $\mathbf{x} \in \mathbb{R}^d$, let $\mathbf{g}_i' = \mathrm{sign}(\hat{\mathbf{g}}_i^{\mathrm{T}}\mathbf{x})\hat{\mathbf{g}}_i$ for $1 \leqslant i \leqslant N$ and $\overline{\mathbf{g}'} = (\sum_{i=1}^{N} \mathbf{g}_i')/N$, then

$$\begin{aligned}\mathbf{x}^{\mathrm{T}}P\mathbf{x} &\geqslant \frac{1}{2N}\sum_{i=1}^{N}\|\mathbf{x} - \mathbf{g}_i'\|^2 \geqslant \frac{1}{2N}\sum_{i=1}^{N}\|\mathbf{g}_i' - \overline{\mathbf{g}'}\|^2 = \frac{1}{4N^2}\sum_{i=1}^{N}\sum_{j=1}^{N}\|\mathbf{g}_i' - \mathbf{g}_j'\|^2 \\ &\geqslant \frac{1}{4N^2}\sum_{i=1}^{N}\sum_{j=1}^{N}\left(1 - \left(\hat{\mathbf{g}}_i^{\mathrm{T}}\hat{\mathbf{g}}_j\right)^2\right).\end{aligned}$$

By equation (15), $\|P^{-1}\| = O(1)$, hence equation (16). □

3.4. Error bounds for the two-step method

Theorem 3.3. *For the two-step method, the error bounds of M and r_c are*

$$\frac{|\delta M|}{M} = \|A_c^+\| O(\epsilon_c), \quad \frac{\|\delta \mathbf{r}_c\|}{a_1} = \frac{R_c}{a_1}\|A_c^+\| O(\epsilon_c), \tag{17}$$

where A_c is the matrix for the quadruple expansion about $\mathbf{r}_c$, and

$$\epsilon_c = \frac{a_1^4}{R_c^4} + \epsilon_n. \tag{18}$$

For a 2D source, the error bounds of $\mathbf{a}$ and U are

$$\frac{\|\delta \mathbf{a}\|}{a_1} = \frac{R_c^2}{a_1^2}\|A_c^+\| O(\epsilon_c), \quad \|\delta U\| = \frac{R_c^2}{a_1^2 - a_2^2}\|A_c^+\| O(\epsilon_c). \tag{19}$$

For a 3D source, the error bounds of $\mathbf{a}$ *and* U *are*

$$\frac{\|\delta\mathbf{a}\|}{a_1} = \frac{R_c^2}{a_1 a_2}\|A_c^+\|O(\epsilon_c), \quad \|\delta U\| = \left(\frac{R_c^2}{a_1^2 - a_2^2} + \frac{R_c^2}{a_2^2 - a_3^2}\right)\|A_c^+\|O(\epsilon_c). \quad (20)$$

Proof. For the multipole expansion about $\mathbf{r}_{c0}$, equation (13) is modified to

$$\|\mathbf{g}_i - \mathbf{g}_Q(\mathbf{r}_i;\mathbf{r}_{c0})\| = \|\mathbf{g}(\mathbf{r}_i)\| \cdot O(\epsilon_{c0}), \quad (21)$$

where $\mathbf{g}_Q(\mathbf{r}_i;\mathbf{r}_{c0})$ is the gravity field at $\mathbf{r}_i$ up to the quadruple term in the multipole expansion about $\mathbf{r}_{c0}$, and

$$\epsilon_{c0} = \frac{\|\mathbf{r}_c - \mathbf{r}_{c0}\|\left(\|\mathbf{r}_c - \mathbf{r}_{c0}\|^2 + a_1^2\right)}{R_{c0}^3} + \frac{a_1^4}{R_{c0}^4} + \epsilon_n.$$

where $R_{c0} = \min_{1\leqslant i\leqslant N}\|\mathbf{r}_i - \mathbf{r}_{c0}\|$. By equation (16), $R_{c0}/R_c = 1 + O((a_1/R_c)^2 + \epsilon_n)$ and $\epsilon_{c0} = O(\epsilon_c)$ with ϵ_c given in equation (18). The rest of the proof is the same as in theorem 3.1 with R, A, and ϵ replaced by R_c, A_c, and ϵ_c respectively. □

4. Numerical simulations

Example 1. We consider noiseless measurements ($\epsilon_n = 0$) around a source with $\mathbf{r}_c \neq \mathbf{0}$. The errors in the source parameters estimated by the quadruple expansion at the origin are given by equations (9)–(12). As we increase the distance from the measuring points to the origin, ϵ in equation (10) varies as R^{-3}. By equations (9)–(12),

$$\begin{aligned} 1\text{-}step: \quad & |\delta M|/M = O\left(R^{-3}\right), \quad \|\delta\mathbf{r}_c\|/a_1 = O\left(R^{-2}\right), \quad \|\delta\mathbf{a}\|/a_1 = O\left(R^{-1}\right), \\ & \|\delta U\| = O\left(R^{-1}\right). \end{aligned} \quad (22)$$

The errors for the two-step method are given by equations (17)–(20). Since ϵ_c in equation (18) varies as R_c^{-4}, and $R_c \approx R$ for $R \gg \|\mathbf{r}_c\|$, we have

$$\begin{aligned} 2\text{-}step: \quad & |\delta M|/M = O\left(R^{-4}\right), \quad \|\delta\mathbf{r}_c\|/a_1 = O\left(R^{-3}\right), \quad \|\delta\mathbf{a}\|/a_1 = O\left(R^{-2}\right), \\ & \|\delta U\| = O\left(R^{-2}\right). \end{aligned} \quad (23)$$

We demonstrate equations (22) and (23) for an ellipse and a rectangular prism.

The ellipse has parameters $\mathbf{r}_c = (0.1, 0.2)$, $\mathbf{a} = (0.4, 0.2)$, and $\alpha_1 = \pi/3$. The gravity fields are measured at three points: $(R, 0)$, $(0, R)$ and (R, R). The exact fields are computed by analytical formulas in [8]. The sources reconstructed by the two methods from the data for $R = 1$ are plotted in figure 1(a). For $R = 1, 2, 4, 8$, the relative errors in M, $\mathbf{r}_c$, $\mathbf{a}$, and U obtained via the quadruple expansion at the origin (one-step) and the two-step algorithm are listed in table 1.

The rectangular prism has parameters $\mathbf{r}_c = (0.15, 0.2, 0.25)$, $\mathbf{a} = (0.5, 0.4, 0.2)$, and U defined by the Euler angles $(\phi, \theta, \psi) = (\pi/2, \pi/4, \pi/2)$. The gravity fields are measured at four points: $(R, 0, 0)$, $(0, R, 0)$, $(0, -R, 0)$, and $(0, 0, R)$. The exact fields are computed by numerical integration. The sources reconstructed from the data for $R = 2$ are plotted in figure 1(b). For $R = 2, 4, 8, 16$, the relative errors in M, $\mathbf{r}_c$, $\mathbf{a}$, and U obtained by the two methods are listed in table 2.

The orders of the relative errors for both sources agree with equations (22) and (23).

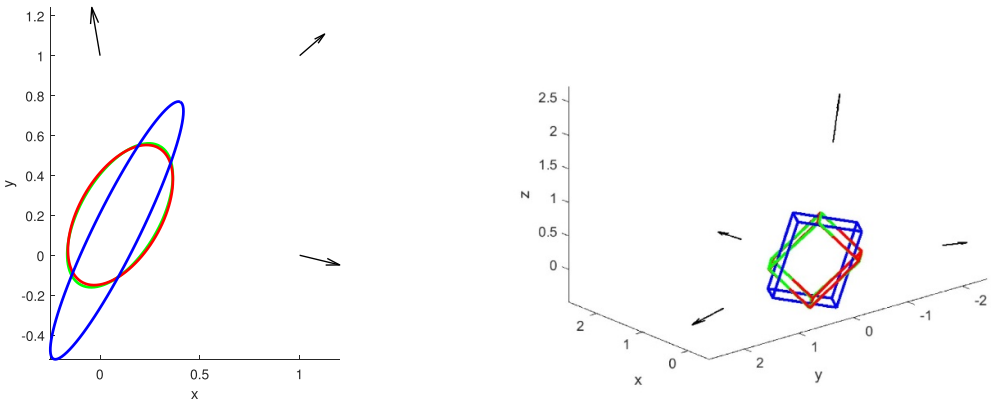

(a) Ellipse (b) Rectangular prism

Figure 1. Example 1. Green: actual source, blue: 1-step method, red: 2-step method, arrows: measured fields. The solution by the 2-step method is very close to the actual source.

Table 1. Example 1 for an ellipse source.

Method	R	$\lvert\delta M\rvert/M$	Order	$\lVert\delta\mathbf{r}_c\rVert/a_1$	Order	$\lVert\delta\mathbf{a}\rVert/a_1$	Order	$\lVert\delta U\rVert$	Order
1-step	1	2.29×10^{-2}	—	1.93×10^{-1}	—	8.23×10^{-1}	—	6.55×10^{-2}	—
	2	2.25×10^{-3}	3.35	3.77×10^{-2}	2.36	3.72×10^{-1}	1.15	5.52×10^{-2}	0.24
	4	2.49×10^{-4}	3.18	8.23×10^{-3}	2.20	1.69×10^{-1}	1.14	3.20×10^{-2}	0.79
	8	2.91×10^{-5}	3.09	1.92×10^{-3}	2.10	7.96×10^{-2}	1.09	1.71×10^{-2}	0.90
2-step	1	8.59×10^{-4}	—	5.71×10^{-3}	—	3.63×10^{-2}	—	2.93×10^{-3}	—
	2	4.37×10^{-5}	4.30	7.36×10^{-4}	2.95	9.91×10^{-3}	1.87	2.04×10^{-3}	0.52
	4	2.33×10^{-6}	4.23	8.72×10^{-5}	3.08	2.51×10^{-3}	1.98	5.25×10^{-4}	1.96
	8	1.34×10^{-7}	4.12	1.05×10^{-5}	3.05	6.25×10^{-4}	2.00	1.29×10^{-4}	2.03

Table 2. Example 1 for a rectangular prism source.

Method	R	$\lvert\delta M\rvert/M$	Order	$\lVert\delta\mathbf{r}_c\rVert/a_1$	Order	$\lVert\delta\mathbf{a}\rVert/a_1$	Order	$\lVert\delta U\rVert$	Order
1-step	2	5.04×10^{-3}	—	4.69×10^{-2}	—	3.14×10^{-1}	—	6.13×10^{-1}	—
	4	7.97×10^{-4}	2.66	1.16×10^{-2}	2.01	1.23×10^{-1}	1.35	3.18×10^{-1}	0.95
	8	1.05×10^{-4}	2.93	2.88×10^{-3}	2.01	5.33×10^{-2}	1.21	1.59×10^{-1}	1.00
	16	1.33×10^{-5}	2.98	7.18×10^{-4}	2.01	2.47×10^{-2}	1.11	7.87×10^{-2}	1.01
2-step	2	1.19×10^{-3}	—	3.58×10^{-3}	—	1.19×10^{-3}	—	3.22×10^{-2}	—
	4	6.77×10^{-5}	4.14	2.94×10^{-4}	3.61	1.61×10^{-3}	−0.44	6.75×10^{-3}	2.25
	8	4.09×10^{-6}	4.05	3.06×10^{-5}	3.26	5.43×10^{-4}	1.57	1.60×10^{-3}	2.08
	16	2.51×10^{-7}	4.02	3.58×10^{-6}	3.10	1.50×10^{-4}	1.86	3.92×10^{-4}	2.03

Example 2. In this example we investigate the effect of the distribution of the measuring points. We assume the measurement are noiseless, and we use the 2-step method. We measure the fields at a few positions near a fixed point P. As the distance from the measuring points to P decreases, $\|A_c^+\|$ increases, while R_c and ϵ_c are essentially fixed. The error bounds in

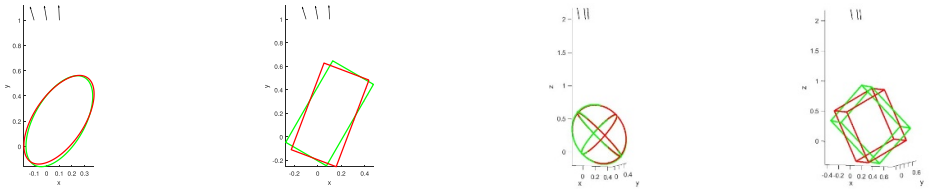

(a) Ellipse (b) Rectangle (c) Ellipsoid (d) Rectangular prism

Figure 2. Example 2 for 3 measuring points with scaling factor $s = 0.1$. Green: actual source, red: reconstructed source, arrows: measured fields.

Table 3. Example 2 for two dimensional sources.

Shape	s	$\|A_c^+\|$	$\|\delta M\|/M$	$\|\delta \mathbf{r}_c\|/a_1$	$\|\delta \mathbf{a}\|/a_1$	$\|\delta U\|$
Ellipse	1	4.56	1.60×10^{-3}	6.10×10^{-3}	1.30×10^{-2}	2.78×10^{-2}
	0.1	162	6.43×10^{-3}	3.00×10^{-2}	8.15×10^{-3}	6.92×10^{-2}
	0.01	1.58×10^{-4}	6.53×10^{-3}	3.05×10^{-2}	1.01×10^{-2}	6.96×10^{-2}
Rectangle	1	4.56	2.92×10^{-4}	3.92×10^{-3}	2.09×10^{-2}	0.031
	0.1	162	5.83×10^{-3}	3.47×10^{-2}	1.85×10^{-2}	0.162
	0.01	1.58×10^{-4}	6.04×10^{-3}	3.60×10^{-2}	1.63×10^{-2}	0.166

equations (17)–(20) increases unboundedly. We demonstrate by 2D and 3D examples that the actual errors are reasonably small even for large $\|A^+\|$.

For the 2D sources, we use the ellipse and the rectangle that share the parameters $\mathbf{r}_c = (0.1, 0.2)$, $\mathbf{a} = (0.4, 0.2)$, and $\alpha_1 = \pi/3$. The gravity fields are measured at three points: $(-s, 1)$, $(0, 1)$ and $(s, 1)$, where s is the scaling factor. The sources reconstructed from the data with $s = 0.1$ are plotted in figures 2(a) and (b). The relative errors for $s = 1, 0.1, 0.01$ are listed in table 3.

For the 3D sources, we use the ellipsoid and the rectangular prism that share the parameters $\mathbf{r}_c = (0.15, 0.2, 0.25)$, $\mathbf{a} = (0.5, 0.4, 0.2)$, and U defined by the Euler angles $(\phi, \theta, \psi) = (\pi/2, \pi/4, \pi/2)$. We consider two cases for each source. In the first case, the fields are measured at 3 points: $(-s, 0, 2)$, $(0, 0, 2)$, and $(s/2, 0, 2)$. The three points are chosen asymmetrically to avoid a singular matrix A (see section 3.2). In the second case, the fields are measured at 5 points: $(0, 0, 2)$, $(-s, 0, 2)$, $(s, 0, 2)$, $(0, -s, 2)$ and $(0, s, 2)$. The sources reconstructed from the data at three points with $s = 0.1$ is plotted in figures 2(c) and (d). The relative errors for $s = 1, 0.1, 0.01$ in all cases are listed in table 4.

The reconstructed sources agree with the actual source qualitatively for clustered points with large $\|A_c^+\|$.

Example 3. In this example we demonstrate the robustness of the two-step method against noise. We perturb the exact fields by a factor of ϵ_n, i.e. $\|\mathbf{g}_i - \mathbf{g}(\mathbf{r}_i)\| = \epsilon_n \|\mathbf{g}(\mathbf{r}_i)\|$, and reconstruct the source from $\{\mathbf{g}_i\}_1^N$. We apply the method to four sources, namely, an ellipse, a rectangle, an ellipsoid, and a rectangular prism. To tolerate noise, we choose the measuring points as in Example 1 for a moderate $\|A_c^+\|$. By equations (18)–(20), the relative errors in $\mathbf{r}_c$, $\mathbf{a}$, and U from noisy measurements are large if $R_c \gg a_1$. For a moderate value of R_c/a_1, we set $R = 1$ for the 2D sources and $R = 2$ for the 3D sources.

Table 4. Example 2 for an ellipsoid source.

Shape	Points	s	$\|A_c^+\|$	$\|\delta M\|/M$	$\|\delta \mathbf{r}_c\|/a_1$	$\|\delta \mathbf{a}\|/a_1$	$\|\delta U\|$
Ellipsoid	3	1	30.7	2.88×10^{-4}	1.92×10^{-3}	2.37×10^{-2}	8.82×10^{-3}
		0.1	4.31×10^{-3}	8.98×10^{-4}	3.56×10^{-3}	2.82×10^{-2}	1.75×10^{-2}
		0.01	4.68×10^{-5}	4.28×10^{-3}	1.09×10^{-2}	2.98×10^{-2}	6.71×10^{-2}
Ellipsoid	5	1	8.10	1.25×10^{-4}	1.05×10^{-3}	1.55×10^{-2}	3.98×10^{-3}
		0.1	685	3.48×10^{-4}	2.46×10^{-3}	2.70×10^{-2}	1.71×10^{-2}
		0.01	6.79×10^{-4}	4.29×10^{-4}	2.71×10^{-3}	2.75×10^{-2}	1.94×10^{-2}
Rectangular Prism	3	1	30.7	7.57×10^{-3}	2.63×10^{-2}	5.27×10^{-2}	0.284
		0.1	4.31×10^{-3}	1.25×10^{-2}	3.90×10^{-2}	6.23×10^{-2}	0.351
		0.01	4.68×10^{-5}	1.32×10^{-2}	4.05×10^{-2}	6.03×10^{-2}	0.352
Rectangular Prism	5	1	8.10	3.81×10^{-3}	1.86×10^{-2}	2.40×10^{-2}	0.214
		0.1	685	4.43×10^{-3}	2.17×10^{-2}	6.09×10^{-2}	0.278
		0.01	6.79×10^{-4}	4.43×10^{-3}	2.18×10^{-2}	6.15×10^{-2}	0.279

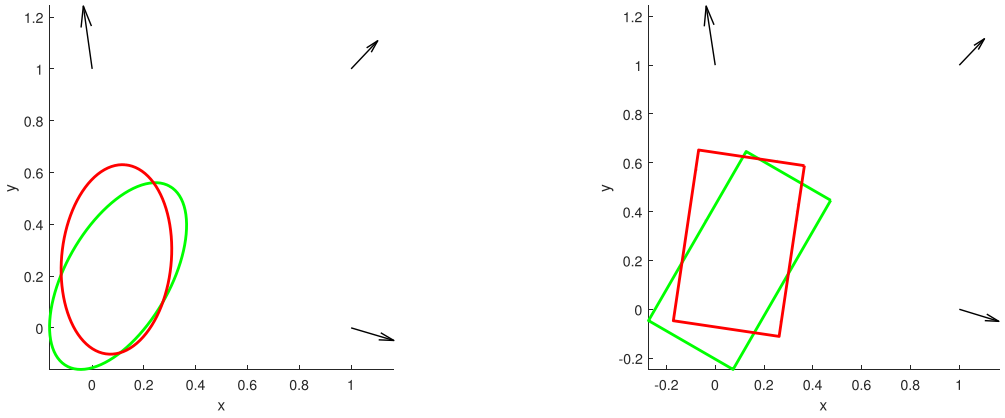

(a) Ellipse (b) Rectangle

Figure 3. Example 3 for 2D sources with 10% noise. Green: actual source, red: reconstructed source, arrows: measured fields with noises.

The ellipse and the rectangle are the same as in example 2. The gravity fields are measured at three points—$(1,0)$, $(0,1)$ and $(1,1)$, for which $\|A_c^+\| = 2.79$. The sources reconstructed from the data with 10% noise are plotted in figure 3. The relative errors for $\epsilon_n = 0, 1\%, 10\%$ are listed in table 5.

The ellipsoid and the rectangular prism are the same in example 2. The gravity fields are measured at four points—$(2,0,0)$, $(0,2,0)$, $(0,-2,0)$, and $(0,0,2)$, for which $\|A_c^+\| = 1.03$. The sources reconstructed from the data with 10% noise are plotted in figure 4. The relative errors for $\epsilon_n = 0, 1\%, 10\%$ are listed in table 6.

The relative errors of the estimated source parameters are reasonably small for measurements with noise up to 10%.

Table 5. Example 3 for two dimensional sources.

Shape	ϵ_n	$\lvert\delta M\rvert/M$	$\lVert\delta\mathbf{r}_c\rVert/a_1$	$\lVert\delta\mathbf{a}\rVert/a_1$	$\lVert\delta U\rVert$
Ellipse	0	8.59×10^{-4}	5.71×10^{-3}	3.63×10^{-2}	2.93×10^{-3}
	1%	6.12×10^{-3}	2.34×10^{-2}	5.88×10^{-2}	7.27×10^{-2}
	10%	2.88×10^{-2}	1.61×10^{-1}	8.76×10^{-2}	4.26×10^{-1}
Rectangle	0	3.38×10^{-3}	1.94×10^{-2}	6.07×10^{-2}	2.56×10^{-2}
	1%	8.69×10^{-3}	3.76×10^{-2}	7.81×10^{-2}	8.15×10^{-2}
	10%	3.21×10^{-2}	1.77×10^{-1}	1.26×10^{-1}	3.74×10^{-1}

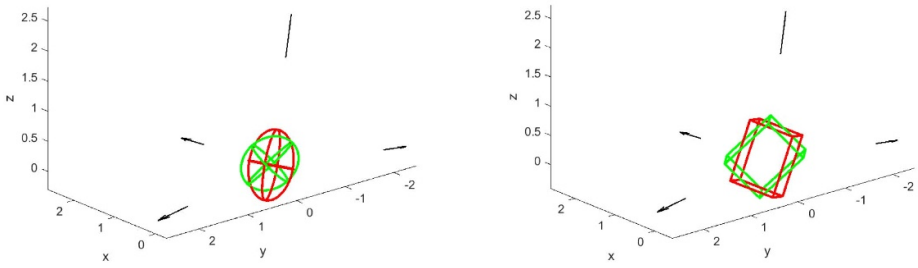

(a) Ellipsoid (b) Rectangular prism

Figure 4. Example 3 for 3D sources with 10% noise. Green: actual source, red: reconstructed source, arrows: measured fields with noises.

Table 6. Example 3 for three dimensional sources.

Shape	ϵ_n	$\lvert\delta M\rvert/M$	$\lVert\delta\mathbf{r}_c\rVert/a_1$	$\lVert\delta\mathbf{a}\rVert/a_1$	$\lVert\delta U\rVert$
Ellipsoid	0	2.79×10^{-5}	1.46×10^{-3}	7.47×10^{-3}	9.86×10^{-3}
	1%	1.08×10^{-2}	6.23×10^{-3}	1.98×10^{-2}	1.17×10^{-1}
	10%	1.10×10^{-1}	6.30×10^{-2}	1.25×10^{-1}	8.90×10^{-1}
Rectangular	0	1.19×10^{-3}	3.58×10^{-3}	1.19×10^{-3}	3.22×10^{-2}
Prism	1%	1.19×10^{-2}	5.39×10^{-3}	1.04×10^{-2}	9.73×10^{-2}
	10%	1.11×10^{-1}	6.08×10^{-2}	6.16×10^{-2}	6.48×10^{-1}

5. Discussion and conclusion

As shown by example 2, the reconstructed source from noiseless measurements is more accurate for elliptic shape than rectangular shape. The reason is that the 16-tuple term in the multipole expansion about the source center divided by the monopole term is $O(a_1^4/R_c^4)$ for rectangles and rectangular prisms, while only $O((a_1^2-\min(a_i)^2)^2/R_c^4)$ for ellipses and ellipsoids, because all terms except the monopole term vanish for a circular (2D) or spherical (3D) source. Therefore, for $\epsilon_n=0$, the term ϵ_c in the error bounds equations (17)–(20) is smaller for an

elliptic source that a rectangular source. On the other hand, in the presence of noises, ϵ_c is dominated by ϵ_n. As shown by example 3, the errors are similar for elliptic and rectangular sources.

In the two-step method, the estimated source center $\mathbf{r}_{c0}$ may be replaced by the approximate source center $\tilde{\mathbf{r}}_c$ obtained by the quadruple expansion about the origin. However, it is not as robust as $\mathbf{r}_{c0}$. By equations (9) and (16), the error of $\tilde{\mathbf{r}}_c$ is at least $R \cdot O(\|\mathbf{r}_c\|^3/R^3 + \epsilon_n)$, while the error of $\mathbf{r}_{c0}$ is $R_c \cdot O(a_1^2/R_c^2 + \epsilon_n)$. For small sources relatively far from the origin ($\|\mathbf{r}_c\| \gg a_1$), $\tilde{\mathbf{r}}_c$ may have a large error, which leads to large errors in the subsequent multipole expansion about $\tilde{\mathbf{r}}_c$.

After the second step in the two-step method, we may use the newly obtained source center, $\mathbf{r}_{c1} = \mathbf{r}_{c0} + \tilde{\mathbf{p}}/\tilde{M}$, as the center of the second multipole expansion. The relative error in the second multipole expansion is still $O((a_1/R_c)^4 + \epsilon_n)$ due to the 16-tuple term, though the octuple term might be smaller because by equations (16) and (17),

$$\|\mathbf{r}_c - \mathbf{r}_{c0}\| = R_c \cdot O\left(\frac{a_1^2}{R_c^2} + \epsilon_n\right), \quad \|\mathbf{r}_c - \mathbf{r}_{c1}\| = R_c \|A_c^+\| O\left(\frac{a_1^4}{R_c^4} + \epsilon_n\right).$$

The error bounds for the source parameters obtained by extra multipole expansions are of the same order as in equations (17)–(20). Therefore, iterative multipole expansions cannot reduce the errors significantly.

In summary, we presented a two-step method of inverse gravimetry. First we back trace the measured gravity fields to estimate the center of the source, then we reconstruct the elliptic or rectangular source by the quadruple expansion centered at the estimated source center. In the second step, we first solve the linear system to determine the approximate monopole, dipole, and quadruple of the source at the center of expansion, then we solve the nonlinear equations for the source parameters exactly.

We proved that the relative errors of the mass, center, half axes, and orientation of the reconstructed source are of 4th, 3rd, 2nd, and 2nd order respectively as the minimum distance between the measuring points and the source center increases. We showed that the minimum number of measuring points is 3 for both two- and three- dimensional sources. Unlike for 2D problems, the linear system for 3D problems may be rank deficient, though it is possible to choose measuring points to make the linear system well-conditioned. For a well-conditioned linear system, the algorithm is robust against noises in the measurements.

Natural underground cavities such as those in karst regions have sophisticated shapes [4]. Recently, a reconstruction method for the inverse gravimetric problem using high order harmonic moments has been proposed in [10]. The authors developed two numerical methods, based on conformal mapping and convex minimization respectively, for two-dimensional cavities. For future work, we will try to extend the method to three-dimensional cavities.

Data availability statement

All data that support the findings of this study are included within the article (and any supplementary files).

Acknowledgments

The research of the authors are supported by the NSF Grant DMS-2008154.

Conflict of interest

The authors state that there is no conflict of interest.

References

[1] Isakov V 1990 *Inverse Source Problems* (American Mathematical Society)
[2] Isakov V, Leung S and Qian J 2011 A fast local level set method for inverse gravimetry *Commun. Comput. Phys.* **10** 1044–70
[3] Beres M, Luetscher M and Olivier R 2001 Integration of ground-penetrating radar and microgravimetric methods to map shallow caves *J. Appl. Geophys.* **46** 249–62
[4] Butler D K 1984 Microgravimetric and gravity gradient techniques for detection of subsurface cavities *Geophysics* **49** 1084–96
[5] Jacob T, Pannet P, Beaubois F, Baltassat J M and Hannion Y 2020 Cavity detection using microgravity in a highly urbanized setting: a case study from Reims, France *J. Appl. Geophys.* **179** 104113
[6] Isakov V, Leung S and Qian J 2013 A three-dimensional inverse gravimetry problem for ice with snow caps *Inverse Problems Imaging* **7** 523–44
[7] Elcrat A, Isakov V, Kropf E and Stewart D 2012 A stability analysis of the harmonic continuation *Inverse Problems* **28** 075016
[8] Isakov V and Titi A 2022 Stability and the inverse gravimetry problem with minimal data *J. Inverse Ill-posed Problems* **30** 147–62
[9] Isakov V and Titi A 2022 On the inverse gravimetry problem with minimal data *J. Inverse Ill-posed Problems* **30** 807–22
[10] Gerber-Roth A, Munnier A and Ramdani K 2023 A reconstruction method for the inverse gravimetric problem *SMAI J. Comput. Math.* **9** 197–225